Heliyon 9 (2023) e21357

Contents lists available at ScienceDirect

Heliyon

journal homepage: www.cell.com/heliyon

Domino index: A rapid quantification tool for the domino effect in chemical plants

Han Gao, Yunkai Yang, Hongxing Shi *

State Key Laboratory of NBC Protection for Civilian, Research Institute of Chemical Defense, Beijing, 102205, China

ARTICLE INFO

Keywords:
Domino effects
Chemical plants
Monte Carlo simulation
Domino index
Risk management

ABSTRACT

The severity of industrial accidents involving domino effects is widely acknowledged in chemical and process industries. The interdependence of installations and complexity of layouts pose significant challenges for the rapid quantitative assessment of domino effects in large chemical plants. In this study, a set of domino indices was introduced to measure the extent to which a given installation triggered and propagated domino effects, as well as to assess the overall domino effect in a specified area. An accelerated algorithm for domino accident modelling was developed based on Monte Carlo simulations to calculate the domino index. This algorithm can simulate all potential domino accident propagation pathways and the failure frequencies of installations. Two case studies, derived for a hypothetical chemical plant and actual oil-storage facilities, were examined to evaluate the applicability of the method. Furthermore, the method was validated using conditional probability calculations and vertex metrics. The results demonstrated that the proposed domino index is a useful tool for rapidly quantifying domino effects and that it can assist in identifying critical installations, designing plant layouts, and screening hazardous areas. The method and indices can provide guidance for the prevention of severe domino accidents.

1. Introduction

Chemical plants typically incorporate numerous interdependent and interconnected installations that contain flammable, explosive, or toxic materials [1]. Moreover, chemical processing industries are becoming increasingly clustered owing to economies of scale [2], leading to a high concentration of hazardous substances. Consequently, a single undesirable incident may propagate to adjacent installations, triggering a series of accidents with overall consequences that are more severe than those of the initial event. This phenomenon is referred to as the 'domino effect' (also known as the cascading failure or knock-on effect).

Domino effects have been widely reported in the literature [3–6]. In the field of industrial safety, accidents involving domino effects generally include the following attributes: (1) a primary event that initiates the domino effect (2) escalation vectors (e.g., thermal radiation, explosion overpressure, and debris projection), that facilitate accident propagation, and (3) one or more secondary events that involve one or more target units [7–9]. Primary accidents include fires, explosions, and toxic releases. Toxic releases are rarely considered in domino effects, as they do not directly damage adjacent facilities. According to Abdolhamidzadeh et al., 43 % of recorded domino events were caused by fires and 57 % were triggered by explosions [10]. Domino effects can typically be divided into three categories: fire-driven, explosion-driven, and fire-and-explosion-driven domino.

Domino effects can be regarded as low-probability, high-impact events [4,11]. Kourniotis et al. [12] investigated 207 major

* Corresponding author.
E-mail addresses: gaohan@sklnbcpc.cn (H. Gao), shihongxing@sklnbcpc.cn (H. Shi).

https://doi.org/10.1016/j.heliyon.2023.e21357
Received 7 June 2023; Received in revised form 10 October 2023; Accepted 19 October 2023
Available online 21 October 2023

accidents and found that 80 were related to domino effects. In December 2005, a series of fires and explosions at an oil storage plant in the Buncefield Complex (UK) led to the largest fire in peacetime Europe, causing 43 injuries and extensive devastation [13]. On March 17, 2019, a chain of fire incidents involving domino effects at Intercontinental Terminals Company (ITC) in Deer Park, Texas, USA, resulted in the failure of seven storage tanks and severe contamination of Tucker Bayou [14]. On March 21, 2019, a massive fire and explosion occurred at a chemical plant in Yancheng, China. The disaster was initially caused by the spontaneous combustion of discarded chemicals, ultimately leading to 78 deaths and 566 injuries [15,16]. The overall consequences of domino accidents are far more severe than those of the primary event. Considering their severity, the risk of domino effects in chemical and process industries should not be neglected, especially for increasingly common chemical clusters.

In the context of safety risk assessment and the management of critical infrastructure, the analysis of domino effects is a pressing concern. Since the 1970s, researchers have extensively investigated domino effects, which can be broadly categorised into two types [17]. The first pertains to the vulnerability of installations, reflecting the capacity of a unit or process plant to initiate or escalate potential domino effects [1]. Various models have been employed in this field, including escalation-threshold methods [18,19], probabilistic methods [20–23], and numerical simulations [24–26]. Escalation-threshold-based methods are convenient but subject to considerable uncertainties in threshold values [3]. Numerical methods such as computational fluid dynamics [27,28] and finite element methods [29] have attracted increasing attention owing to their ability to simulate physical effects. However, these methods require considerable computational resources [26]. Probabilistic methods are commonly used; they can manage uncertainties in domino effects and are well suited for quantitative risk assessment [30].

The second type entails modelling of the evolution of domino effects. Lower-order domino accidents can damage multiple installations in parallel, whereas installations involved in higher-order accidents may incur damage from multiple sources [4,31]. Modelling domino accidents while considering spatiotemporal and synergistic effects is challenging. Available methods include Bayesian networks [32–34], vertex metrics [13,35,36], and stochastic simulation methods [10,37,38].

Approaches for modelling the evolution of domino accidents are typically employed in the consequence assessment and risk analysis of chemical plants. However, these methods are complex and time-consuming, particularly for plants with numerous installations [39]. Therefore, indicators that facilitate the rapid quantification of domino effects and identification and preliminary ranking of critical installations in large chemical plants are urgently required. These quantitative indicators should encompass two aspects: (i) a single installation (node) and (ii) an area containing multiple installations (system). Research on this topic has been limited. Cozzani et al. [40] proposed a set of hazard indices for identifying and ranking critical units in process plants. Khakzad et al. [41] developed a Bayesian network methodology to determine the most probable sequence of accidents in a process plant. Reniers and Audenaert [42] employed a network theory approach to identify and rank the most vulnerable intermediate and terminal units in process systems by utilising 'terminal and propagation vulnerability indices'. Khakzad et al. [11] investigated the effectiveness of a set of vertex metrics for evaluating domino effects within process plants. Metrics such as degree, closeness, and betweenness were found to be useful for determining critical units and identifying the most vulnerable plant layouts. However, these methods primarily focus on the plant layout and escalation vectors when characterising domino effects, and they do not include the evolution of domino accidents or adequately reflect the potential consequences of domino scenarios. Thus, there is a need for a rapid quantification tool that encompasses accident propagation simulations, to assess domino effects in process plants and thereby support risk-management efforts in chemical parks.

Motivated by this need, we herein introduce a series of domino indices, including the domino impact score, domino propagation score, element domino index, and system domino index. To obtain these indices, an accelerated domino accident modelling method based on Monte Carlo simulations is also proposed, which can simulate all potential domino accident propagation pathways and installation failure frequencies. The method and indices were designed to measure the extent to which a given installation could trigger and propagate a domino effect, as well as to assess the overall domino effect in a specified area. Applications may include the identification of hazardous installations, layout design, and the screening of chemical plants for risk management.

The paper is structured as follows. The accelerated algorithm for domino effect modelling is described in Section 2. Section 3 defines the set of domino indices and briefly introduces their applications. In Section 4, the application of domino indices to identify the most critical initiating and transmitting units in a hypothetical chemical plant is described. Section 5 presents a case study of five existing oil-storage plants and describes the methodology for quantifying and ranking the overall domino effects in different plants. In Section 6, the results obtained from the application of domino indices are compared with those obtained from conditional probability calculations and the vertex metric methodology. Furthermore, the contributions and limitations of the method are discussed. Finally, the main conclusions of the study are presented in Section 7.

2. Modelling of domino effects

Domino effects often encompass multiple accident chains that proceed in series or parallel and are considerably more complex than a single-accident escalation. The probit model is frequently employed to simplify accident escalation modelling in quantitative analyses of domino effects [43]. However, the application of probit models to large chemical plants requires extensive and complex probability calculations [44]. In this section, we introduce an accelerated method for domino accident modelling, based on Monte Carlo simulations. Using a specific number of stochastic simulations, the Monte Carlo method can effectively model uncertainties in the propagation of escalating vectors within chemical plants. The outcomes of the stochastic simulations serve as inputs for calculating the domino indices in subsequent stages.

Notably, the domino indices presented in this paper primarily pertain to the state and layout of a chemical plant, with less emphasis placed on the cause and frequency of the initial accidents.

2.1. Plant information and installation data

The first step involves gathering information and data required to implement the simulation method in a chemical plant. Three types of information are collected: (i) plant information, (ii) installation data, and (iii) the hazard level of the installations. These data can be explained as follows.

(i) Plant information: The layout of the plant (with installation coordinates) and environmental information (e.g., atmospheric stability and common wind speeds and directions).
(ii) Installation data: Types and geometric parameters of the installations, as well as the substances involved (types and quantities).
(iii) Hazard level: The potential hazards associated with different installations, as characterised using the classification indicator for major hazards [45]:

$$f = \frac{\beta q}{Q}, \tag{1}$$

where f denotes the hazard level of the installations, β is the correction factor for the material used in the installation, q is the actual quantity of material (in tonnes), and Q is the threshold quantity of the material (in tonnes).

2.2. Calculating escalation probabilities

The calculation of escalation vectors for different installations is a prerequisite to accident propagation modelling. In the event of an explosion, the overpressure exerted from one installation to another can be calculated using models such as the TNT equivalent, compound energy, or Baker–Strehlow–Tang methods, as well as using commercial software such as DNV Phast. A matrix OP can be created for the escalation vectors of the overpressure, as

$$OP = \begin{bmatrix} 0 & p_{12} & \dots & p_{1n} \\ p_{21} & 0 & \dots & p_{2n} \\ \dots & p_{ij} & 0 & \dots \\ p_{n1} & p_{n2} & \dots & 0 \end{bmatrix}, \tag{2}$$

where p_{ij} is the overpressure on the j-th installation in the event of an explosion at the i-th installation. If $j = i$, $p_{ij} = 0$.

The probit model [20,46] was adopted to calculate the escalation probability P, as

$$P = \frac{1}{\sqrt{2\pi}} \int_{-\infty}^{Pr-5} e^{-\frac{x^2}{2}} dx, \tag{3}$$

where Pr is the probit unit determined by the overpressure and type of target installation. Pr is obtained from

$$Pr = k_1 + k_2 \ln(p_s), \tag{4}$$

where p_s denotes the peak static overpressure (Pa). For atmospheric installations, $k_1 = -18.96$ and $k_2 = 2.44$; for pressurised installations, $k_1 = -42.44$ and $k_2 = 4.33$.

For the fire-driven domino effect, the probit unit is calculated as follows [21,29]:

$$Pr = 9.25 - 1.85\, ln(ttf), \tag{5}$$

where ttf is the time to failure (in minutes), which represents the resistance of the target equipment to an external fire. The ttf can be estimated as

$$ln(ttf) = \alpha\, ln(Q) + \beta. \tag{6}$$

For atmospheric installation, $\alpha = -1.128$ and $\beta = -2.667 \times 10^{-5} \times V + 9.877$..

For pressurised installation, $\alpha = -0.947$ and $\beta = 8.835 \times V^{0.032}$..

Here, Q denotes the thermal radiation received by the installation (kW/m^2) and V denotes the installation volume (m^3). The unit of ttf is seconds.

Thus, the escalation vectors of overpressure and thermal radiation can be converted into escalation probabilities to obtain

$$EP = \begin{bmatrix} 0 & g_{12} & \dots & g_{1n} \\ g_{21} & 0 & \dots & g_{2n} \\ \dots & g_{ij} & 0 & \dots \\ g_{n1} & g_{n2} & \dots & 0 \end{bmatrix}, \tag{7}$$

where g_{ij} denotes the probability of an accident in the i-th installation escalating towards the j-th installation.

2.3. Monte Carlo simulation

This step simulates the actual behaviour of a multi-unit system under potential domino effects. A chemical plant and its installations can be represented using a fully weighted graph (G) [35]. The graph is expressed by

$$G = (V, E, f, g), \tag{8}$$

$$V = \{V_1, V_2 \dots V_i, \dots, V_n\}, \tag{9}$$

$$E = \{E_{12}, E_{13} \dots E_{ij} \dots\}, \tag{10}$$

$$f = \{f_1, f_2, f_3 \dots f_n\}, \tag{11}$$

$$g = \{g_{12}, g_{13} \dots g_{ij} \dots\}, \tag{12}$$

where V represents a set of nodes (elements) that represent installations in a chemical plant, and V_i represents the i-th installation. E represents the set of directed edges from the installations that produce escalation vectors (V_i) to the target installations (V_j). f is a group of node weights, and f_i is the hazard level of the installations obtained using Eq. (1). g is a group of edge weights, and g_{ij} denotes the escalation probability from V_i to V_j. Nodes do not necessarily interact with one another. The results of the Monte Carlo simulations are the frequencies of the node failures in system. A flow diagram of the algorithm is shown in Fig. 1.

Step 1. Abstract the plant as a graph model by Eqs. (8)–(12). Calculate the escalation vectors and escalation probabilities between the nodes. Specify the number of iterations (N). The parameter *Repeat* is a counter and represents the number of iterations. It is initialised to one.

Step 2. To investigate node V_i, identify the set of all directed edges starting from it $E_i = \{E_{i1}, E_{i2}, E_{i3} \dots\}$ and the corresponding escalation probabilities $g_i = \{g_{i1}, g_{i2}, g_{i3} \dots\}$. For a specific directed edge E_{ij} and corresponding escalation probability g_{ij}, generate a

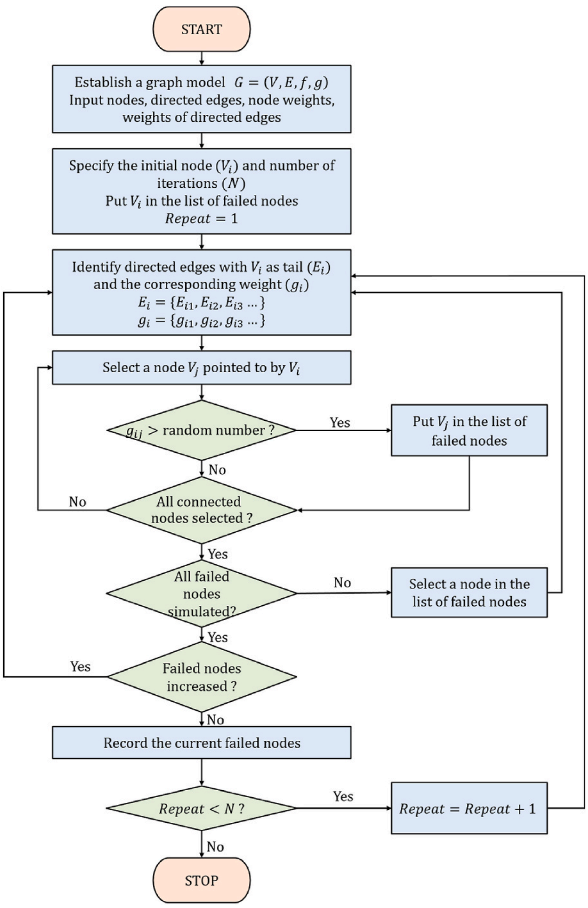

Fig. 1. Flow diagram of the accelerated algorithm based on Monte Carlo simulations.

random number that is uniformly distributed between 0 and 1. Compare the random number with the escalation probability g_{ij}. If the random number is smaller than g_{ij}, the target installation V_j is considered to have failed and is included in the list of failed nodes. This is the first level of domino effect propagation.

Step 3. For installations $V_{k_1}, V_{k_2}, V_{k_3}\ldots$ in the failed node list, identify the set of all directed edges starting therefrom, as well as the corresponding escalation probabilities. Each identified escalation probability is compared to a generated random number. If the random number is smaller than the escalation probability, the corresponding node is considered to have failed. This is the second level of domino effect propagation.

Step 4. For installations that fail in the second level of the domino effect, $V_{l_1}, V_{l_2}, V_{l_3}\ldots$, perform Monte Carlo simulations as in Steps 1 and 2 to model higher-level domino effect propagation. The single simulation trial terminates when no new failures occur.

Step 5. A round of execution of Steps 2–4 is considered one iteration. Repeat Steps 2–4 until the pre-set number of iterations is reached.

Step 6. Record all the failed installations in the final scenario; this serves as the domino accident model for V_i.

3. Domino indices

The element domino index (*EDI*) has been proposed to rapidly identify installations with significant domino effects in chemical plants. Based on this concept, we introduce an index for specific areas: the system domino index (*SDI*). This section presents the definitions and applications of these indices.

3.1. Element domino index

The *EDI* represents the hazard related to domino effects initiated and transmitted by a given installation. It includes two factors: the domino impact score (*DIS*) and domino propagation score (*DPS*). The former implies an eventual hazard resulting from the domino effect triggered by a given installation; the latter reflects the contribution of the propagating domino effects for a given installation as a component of the accident chain. The *DIS* and *DPS* are defined as follows:

The DIS_i of Node V_i is defined as the expected value of the sum of the failed node weights in the final scenario, assuming that the failure of node V_i is a primary accident, and it is expressed as

$$DIS_i = \sum_{j\neq i}^{n} f_j \bullet P_{ji} = \frac{1}{N}\sum_{j\neq i}^{n} f_j \bullet Freq_{ji}, \tag{13}$$

where P_{ji} and $Freq_{ji}$ denote the probability and frequency of V_j failure, respectively, given V_i failure as the initial event. N indicates the number of Monte Carlo simulations. f_j is the weight of V_j (i.e., the hazard level of the installation), and n is the number of nodes.

The DPS_i of V_i is a measure of the contribution of node V_i to the transmission of domino effects. Qualitatively, the contribution is significant when node V_i is located at the hub for a given layout. This study quantifies this contribution as the amplification of domino effects attributable to the presence of V_i when other nodes in the system fail as an initial event as follows:

$$DPS_i = \frac{1}{n-1}\sum_{j\neq i}^{n}\left(DIS_j - \overline{DIS}_{ji} - \frac{f_i \bullet Freq_{ij}}{N}\right), \tag{14}$$

where DIS_j is the domino impact index of node V_j, and $\overline{DIS}_{ji}$ is the domino impact index of node V_j when node V_i is removed from the graph. $Freq_{ij}$ is the frequency at which node V_i fails when node V_j fails as the initial event.

$DIS_j - \overline{DIS}_{ji}$ quantifies the magnification of the domino effect in the presence of V_i. However, DIS_j also includes the contribution of V_i owing to its failure. Therefore, the corresponding component, $f_i \bullet Freq_{ij}/N$, must be subtracted.

The *EDI* consists of *DIS* and *DPS*, as shown in the following equation:

$$EDI_i = DIS_i + DPS_i \ . \tag{15}$$

3.2. System domino index

The *SDI* represents the overall domino effect within a system. It incorporates the characteristics of all nodes and emphasises the nodes where the domino effect is significant. In this study, the generalised mean of the EDI_i in the system was used to define the *SDI* as follows:

$$SDI = \left(\frac{1}{n} \bullet \sum_{i=1}^{n} EDI_i^{\,p}\right)^{\frac{1}{p}}, \tag{16}$$

where p denotes a predefined parameter. When $p = 1$, *SDI* is the average of all EDI_i. The larger the value of p, the greater the dependence of the *SDI* on the larger value of the EDI_i, which was chosen as 2 in this study.

A script was written in Python 3.11 that integrated Monte Carlo simulations and the calculation of domino indices. The domino indices can be obtained by simply entering the required information.

3.3. Application of domino indices

(1) Identification of critical installations

The higher the *DIS*, the more severe the consequences of a primary accident at the installation. Installations in a chemical plant can be ranked according to the *DIS*, and those with significantly high *DIS* values can be identified. Risk-management measures including increased safety supervision, reinforced safety barriers, and accelerated emergency responses can be implemented to reduce the likelihood of primary accidents at critical installations. The *DPS* was applied in a manner similar to the *DIS*. The identification of installations with significant impacts and transmission capabilities is crucial for the allocation of resources when the investment in safety is limited.

(2) Optimisation of plant layout

The domino effect is an important consideration in the design of industrial layouts [47]. The *SDI* can be used to rapidly characterise the hazards of domino effects for a given plant layout. The preliminary design of the layout can be optimised to decrease the *SDI*. Several alternative designs can be ranked using the *SDI*.

(3) Screening for domino effects in chemical plants

The proposed domino indices facilitate the rapid quantification and dynamic simulation of accident propagation, which facilitates rapid risk screening for numerous existing chemical plants using the *SDI*. A higher *SDI* indicates more severe consequences that involve domino effects. For plants with a high *SDI* in a chemical cluster, factory managers should coordinate and integrate safety resources to mitigate the consequences of accidents. In addition, plants with high *SDIs* are also more susceptible to terrorist attacks; thus, the *SDI* should be considered when evaluating security resources. Table 1 summarises the definitions, interpretations, and applications of domino indices.

4. Case study 1: A single plant

4.1. Description of the case

The objective of Case Study 1 was to demonstrate the application of the *EDI*. A chemical storage area containing six storage tanks is shown in Fig. 2. T1 and T2 are atmospheric installations, each containing 50 tonnes of nitrobenzene. T3–T6 are pressurised installations containing liquefied propane. Nitrobenzene has a propensity to explode, and boiling liquid-expanding vapour explosions (BLEVEs) may occur in storage tanks containing liquefied propane. Chemical explosions and BLEVE were assumed the only accident types for T1–T2 and T3–T6, respectively. Therefore, the type of domino effect in this case was explosion-driven domino. Atmospheric effects were not considered because both the nitrobenzene explosion and BLEVE are instantaneous. The characteristics of the storage tanks are summarised in Table 2. In this case study, the TNT equivalent method and DNV Phast 8.0 software were adopted to calculate the overpressure associated with the nitrobenzene explosion and BLEVE, respectively. In addition, the threshold amounts of liquefied propane and nitrobenzene were 50 and 10 tonnes, respectively [45], and the hazard level was calculated using Eq. (1). Notably, in this case, no threshold was set for the escalation vector; in fact, if the target installation is subjected to insufficient overpressure, the escalation probability will be negligibly low.

Table 1
Domino indices proposed in this study.

Index name	Domino impact score	Domino propagation score	Element domino index	System domino index
Acronym	*DIS*	*DPS*	*EDI*	*SDI*
Definition	Eq. (13)	Eq. (14)	Eq. (15)	Eq. (16)
Range of values	> 0	> 0	> 0	> 0
Interpretation	Measure of the hazards related to domino effects initiated by a given installation	Measure of the contribution of a given installation to the transmission of domino effects	Sum of *DIS* and *DPS* for an installation	Measure of the overall hazard related to domino effects in a given plant or area
Application	Identification of critical escalation sources	Identification of pivotal escalation intermediaries	Hazard ranking of installations in a plant or area	Optimisation of plant layout; preliminary risk screening

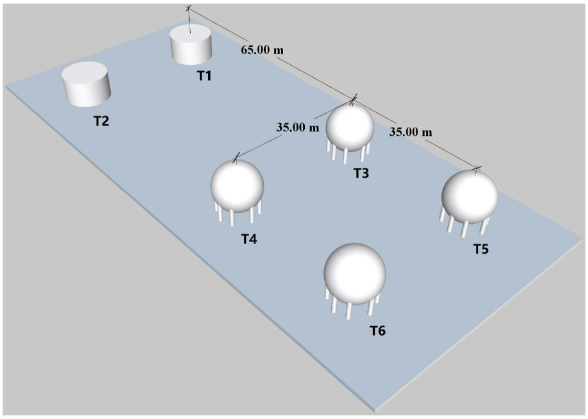

Fig. 2. Layout of the six storage tanks used in Case Study 1.

Table 2
Features of chemical storage tanks in Case Study 1.

Tank No.	Type of tanks	Substance	Inventory (t)	Threshold amount (t)	Hazard level *f*
T1	Atmospheric	Nitrobenzene	50	10	10
T2	Atmospheric	Nitrobenzene	50	10	10
T3	Pressurised	Liquefied propane	50	50	2
T4	Pressurised	Liquefied propane	50	50	2
T5	Pressurised	Liquefied propane	100	50	4
T6	Pressurised	Liquefied propane	100	50	4

4.2. Results and discussion

Using Eqs. (2)–(4), the obtained escalation vectors can be converted into escalation probabilities, the results of which are listed in Table 3. The overpressures released by the explosion of T1 and T2 considerably exceeded those of the BLEVEs for T3–T6. The escalation probabilities of T1→T2 and T2→T1 reached a value of 1. However, the damaging effect of T1 and T2 on the pressurised storage tanks (T3–T6) was insignificant, and the escalation probabilities were all below 0.34. However, the probabilities of T1 and T2 failures owing to the pressurised tanks remained considerable. This may be because pressurised tanks are more resistant to overpressures than atmospheric tanks, which is also reflected in the probit models for different types of installations.

As shown in Table 2, T1 and T2 had the highest hazard level, while T5 and T6 had the largest inventory. T3 and T4 were located in the middle of the plant layout, which was conducive to the spread of domino effects. Therefore, directly identifying critical installations relevant to the domino effect using the abovementioned information was difficult.

The proposed method was used to quantify domino effects in plants. The statistical results of the Monte Carlo simulations for *DIS* are shown in Table 4 (10,000 simulations). The mean of the simulation values is the *DIS* of the corresponding tank. Table 5 is a summary of the domino indices. In this case, the domino indices of the tanks in symmetrical positions are essentially identical. T5 and T6 exhibited the highest *DIS*, which indicated that they had the highest probability of triggering domino effects. Therefore, such installations are highly susceptible to terrorist attacks. In security and risk management, more safety and security resources should be allocated to these installations, with a priority on reducing the likelihood of primary incidents. In addition, T3 and T4 exhibited the highest *DPS*, which may have been attributable to the locations of T3 and T4 in the middle of the region. Safety measures should be highlighted to interrupt edges directed toward other installations. The case study also shows that installations with the highest *DIS* and *DPS* do not necessarily overlap.

Monte Carlo simulations were used to model the propagation of domino accidents in the proposed domino indices. The theoretical values of the Domino indices were approximated based on a specific number of repeated simulations. To determine the appropriate

Table 3
Escalation probabilities from T_i to T_j in Case Study 1.

$T_i \backslash T_j$	T1	T2	T3	T4	T5	T6
T1	0	1	0.334	0.083	0	0
T2	1	0	0.083	0.334	0	0
T3	0.603	0.413	0	0.389	0.389	0
T4	0.413	0.603	0.389	0	0	0.389
T5	0.29	0.225	0.818	0.115	0	0.818
T6	0.225	0.29	0.115	0.818	0.818	0

Table 4
The statistical data for Monte Carlo simulations.

	Mean	Maximum	Minimum	Standard deviation	95 % confidence interval
T1	14.464	22	10	4.891	(14.368, 14.560)
T2	14.558	22	10	4.936	(14.461, 14.655)
T3	22.935	30	0	8.886	(22.761, 23.109)
T4	23.128	30	0	8.660	(22.958, 23.298)
T5	26.031	28	0	5.556	(25.922, 26.140)
T6	25.921	28	0	5.691	(25.809, 26.033)

Table 5
Domino indices of T1–T6 (number of simulations: 10,000).

	T1	T2	T3	T4	T5	T6
DIS	14.464	14.558	22.935	23.128	26.031	25.921
DPS	1.922	1.896	2.027	1.990	1.421	1.471
EDI	16.386	16.454	24.962	25.118	27.452	27.392
SDI	23.44					

number of simulations, *EDI* and *SDI* were calculated for $N = 1$; 10; 100; 1000; 5000; 10,000; and 20,000. The results are shown in Fig. 3. Fig. 3a shows the effect of the number of simulations on the *EDI*. When the number of simulations was small, the *EDI* fluctuated considerably. When the number of simulations approached 1000, the *EDI* values of the tanks in the symmetrical position coincided, and the values stabilised. Fig. 3b shows the effect of the number of simulations on the *SDI*, where the yellow polyline denotes the relative error (assuming that the *SDI* obtained for $N = 20,000$ is the true value). The relative errors were below 0.01 when N exceeded 1000. Therefore, 1000 simulations were considered in the case study. Under these conditions, 3.57 s was required to calculate the domino index of all the storage tanks (Intel i7-12700 CPU). Thus, the proposed rapid quantification tool is convenient and expeditious.

5. Case study 2: Five existing storage plants

5.1. Description of the case

In this case study, five existing large-scale storage plants were considered. Fig. 4(a–e) illustrate the layouts of Plants 1–5, respectively, with the separation distances between the tanks specified. Each plant contained more than 20 tanks, and a catastrophic accident in any one tank could trigger a domino effect, potentially leading to severe consequences. The domino index enables the rapid analysis and classification of complex chemical plants with numerous installations. This section demonstrates the use of the domino index to assess domino effects in chemical plants with complex layouts. The tanks in different plants shared similar characteristics, enabling a direct demonstration of the influence of the plant layout on the domino effects. The stored substance was crude oil, and the type of accident was assumed a pool fire. Hence, the type of domino effect in these plants was fire driven. The basic features of the tanks are listed in Table 6.

Before executing the Monte-Carlo-simulation-based algorithm, the Mudan model [16,48] was used to obtain the thermal radiation of the pool fires as follows:

$$q(r) = \frac{D \bullet \Delta H_c \bullet m_f \bullet f}{D + 4H} \bullet [1 - 0.0581\ ln(r)] \bullet V \tag{17}$$

where D is the equivalent diameter (m), H is the height of the flame, q_0 is the thermal radiation of the flame (kW/m^2), r is the distance

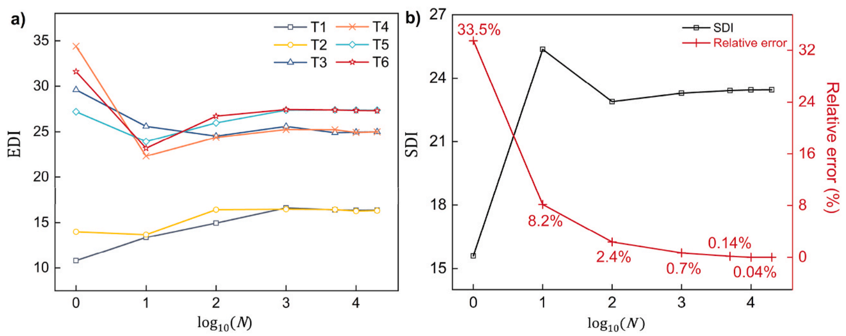

Fig. 3. Effect of number of simulations on (a) *EDI* and (b) *SDI*.

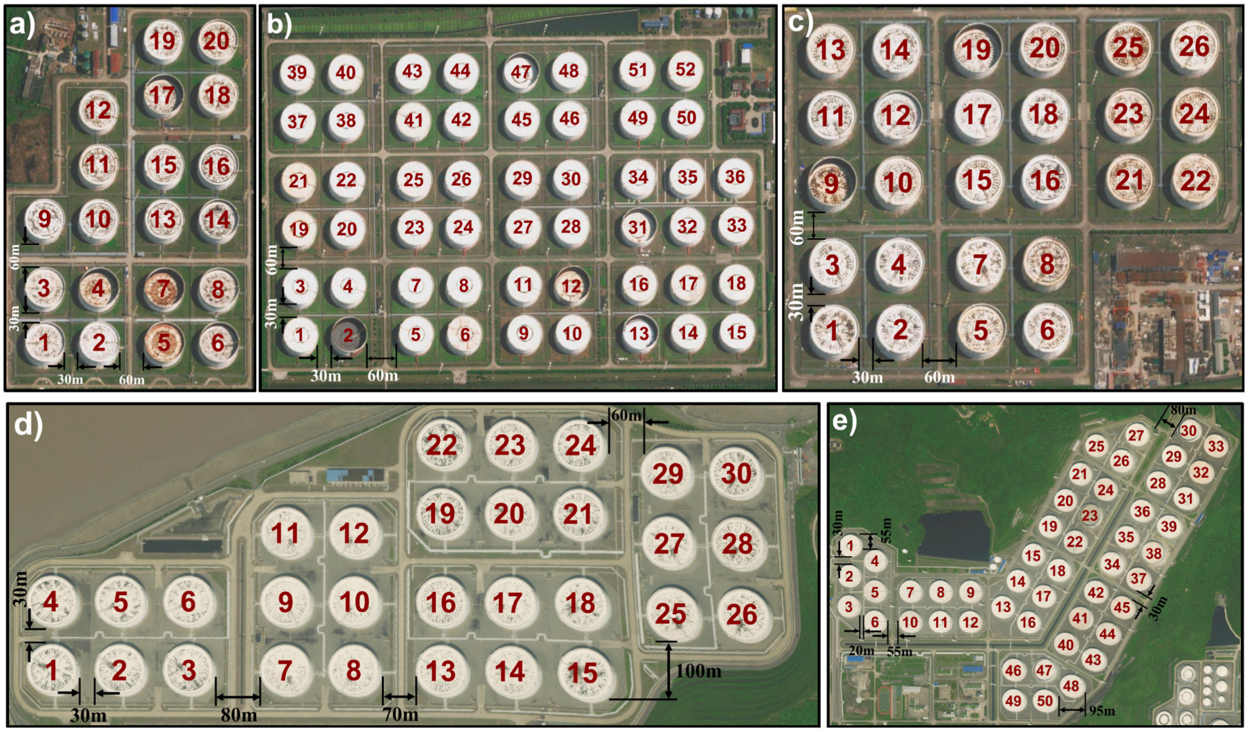

Fig. 4. Layouts of five existing storage plants: (a) Plant 1, (b) Plant 2, (c) Plant 3, (d) Plant 4, and (e) Plant 5.

Table 6
Basic features of the tanks used in Case Study 2.

Plant	Tanks	Diameter (m)	Height (m)	Type	Substance	Hazard level	Combustion heat (kJ/kg)	Burning rate (kg/m^2·s)
Plant 1	T1-T20	80	21.8	Atmospheric	Crude oil	200	41870	0.017
Plant 2	T1-T52	80	21.8	Atmospheric	Crude oil	200	41870	0.017
Plant 3	T1-T26	80	21.8	Atmospheric	Crude oil	200	41870	0.017
Plant 4	T1-T30	80	21.8	Atmospheric	Crude oil	200	41870	0.017
Plant 5	T1-T50	80	21.8	Atmospheric	Crude oil	200	41870	0.017

from the centre of the fire (m), ΔH_c is the heat of combustion (kJ/kg), f is the thermal radiation coefficient, generally 0.15, and m_f is the burning rate (kg/m^2·s). V is the view factor, which was calculated using a previously published method [49]. After obtaining the escalation vectors using Eq. (17), the escalation probabilities were calculated according to Eqs. (3) and (5)–(7).

5.2. Results and discussion

Fig. 5(a–e) show the element domino indices of the tanks in Plants 1–5, respectively. The tanks were classified and marked using distinctive colours according to the *EDI* values. The results revealed that the tanks situated closer to the central area exhibited higher *EDIs*, which implied an increased propensity of these tanks to inflict damage on adjacent tanks. As described in Section 5.1, enhanced safety resources could be allocated to these installations.

Safety resource allocation and risk management are typically operated regionally, which requires the quantification of plant-wide domino effects. Generally, the more tanks in a given plant, the more pronounced the potential domino effect. In this case study, Plants 1–5 included numerous tanks containing hazardous materials and exhibiting complex layouts. The *SDI* was used to quantify the domino effects across these plants, and the results are illustrated in Fig. 6. Plant 2 exhibited the highest *SDI*. Although the number of tanks in Plant 5 was comparable to that in Plant 2 (52 in Plant 2 and 50 in Plant 5), the *SDI* was notably smaller (260.71 in Plant 2 and 215.78 in Plant 5), which may be attributed to the more concentrated layout of Plant 2. Similarly, Plants 3 and 4 had 26 and 30 tanks, respectively. However, the former exhibited a higher *SDI* than the latter (203.73 and 176.02, respectively). These findings demonstrate the influence of regional layouts on the *SDI*.

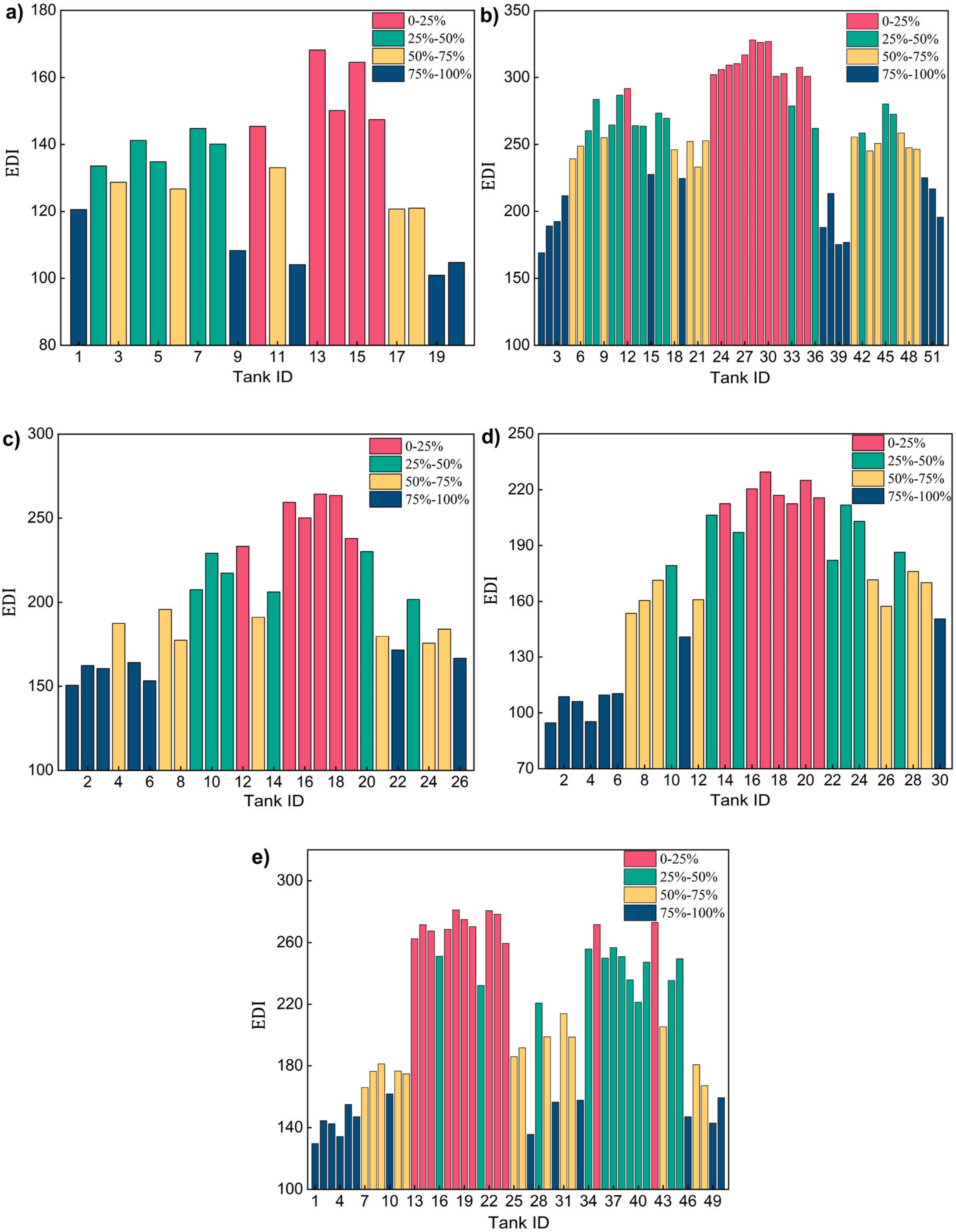

Fig. 5. *EDI* values of tanks in five storage plants: (a) Plant 1, (b) Plant 2, (c) Plant 3, (d) Plant 4, and (e) Plant 5.

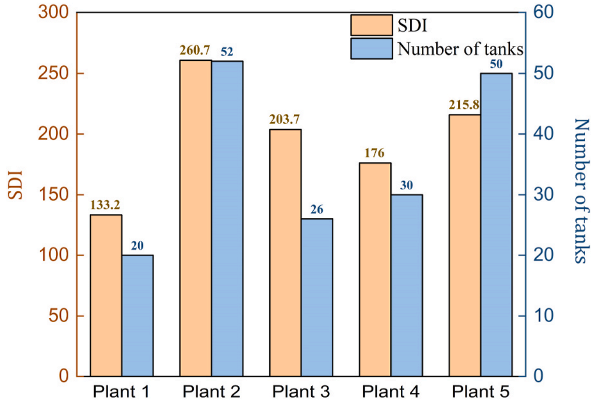

Fig. 6. *SDI* and number of tanks in the five storage plants.

6. Validation and discussion of methodology

The domino indices proposed in this study facilitate the modelling of domino accidents. To this end, an accelerated algorithm for domino accident modelling, based on Monte Carlo simulations, was introduced. To validate the effectiveness of the method, a comparison was made with the method proposed by Cozzani et al. [46]. Considering the *DIS* calculation in Case Study 1 as an example, when calculating the *DIS* of T3, the explosion of T3 was the primary event. In the final accident scenario, each adjacent tank had two states, failure or non-failure, resulting in $2^5–1 = 31$ final accident scenarios. Multiple domino accident propagation paths were available for each final accident scenario. For instance, if the failures of T1, T3, and T4 constituted the final accident scenario, the possible accident propagation paths would be as follows: (1) T3 caused T4 failure, which subsequently escalated to T1 failure; (2) T3 caused T1 failure, which led to T4 failure; and (3) T3 simultaneously caused T1 and T4 failures. Therefore, analysing domino effects in large-scale chemical plants using conditional probabilities is exceedingly challenging.

The case scenario was further simplified to three tanks (T3–T5). A simplified layout is depicted in Fig. 7. According to the method described by Cozzani et al. [46], when a primary accident occurred at T3, four possible domino accident propagation paths were available: (1) T3 caused T4 failure, (2) T3 caused T5 failure, (3) T3 simultaneously caused T4 and T5 failures, and (4) T3 first caused T5 failure, which then caused T4 failure. Notably, Paths 1–3 represent the first-level domino effect, whereas Path 4 represents the second-level effect. By calculating the probabilities of each domino accident path, the *DIS* of T3 can be obtained, as shown in Table 7. The accelerated algorithm for domino accident modelling was also employed to calculate the *DIS* of T3. A discrepancy of only 0.2 % was obtained between the results for the two methods (2.384 for the proposed method and 2.389 for that of Cozzani et al.), which validates the effectiveness of the algorithm for quantifying domino effects.

Khakzad and Reniers [1,13] employed graph theory and vertex metrics to evaluate the domino effects of process plants. The vertex metrics used were betweenness and closeness. The betweenness of a vertex is defined as the fraction of geodesic distances between all pairs of vertices that traverse the vertex of interest, which reflects the contribution of the vertex-transmitting domino effects. The closeness of a vertex is the number of steps required to reach every vertex in the graph from a given vertex, which represents the potential capacity of the vertex to produce escalation. Consequently, betweenness can be compared to the *DPS*, whereas closeness can be compared with the *DIS* proposed in this study.

The case study presented by Khakzad and Reniers [1] was discussed. A storage plant with eight atmospheric storage tanks containing benzene was considered, as shown in Fig. 8. All tanks had a capacity of 200 m^3, and the prevailing wind was southeast at 5 m/s. Pool fires were considered the only accident scenario. In this study, the thermal radiation intensities, which have been described in the literature, were used to calculate the domino indices.

The domino indices of the plants were computed from the escalation vectors. For comparison, the vertex metrics for the tanks, as cited in the literature, are listed in Table 8. Fig. 8 shows that T6 and T8 interacted with most of the tanks via directed edges, resulting in the highest closeness (0.0548). The results for the domino index showed that T6 and T8 had the highest *DIS* (14.5). T5, situated at the centre of the graph, puts out three escalation vectors and received two. The results of the vertex metrics indicated that T5 possessed the highest betweenness (3.87). The *DPS* of T5 was also the highest (1.36) owing to its central position. In conclusion, the domino indices and vertex metrics yielded congruent rankings of tanks related to the domino effects within the storage plant.

The aforementioned examples demonstrate the validity of the domino index for quantifying the domino effect. The main contributions of the proposed index are as follows.

(1) The proposed domino index dynamically models accident propagation processes.
(2) The Monte-Carlo-simulation-based method accelerates domino accident modelling and indicates expediency in quantifying domino effects in large-scale plants (it required less than 4 s for Case Study 1). This attribute may potentially facilitate widespread acceptance and implementation of the method.

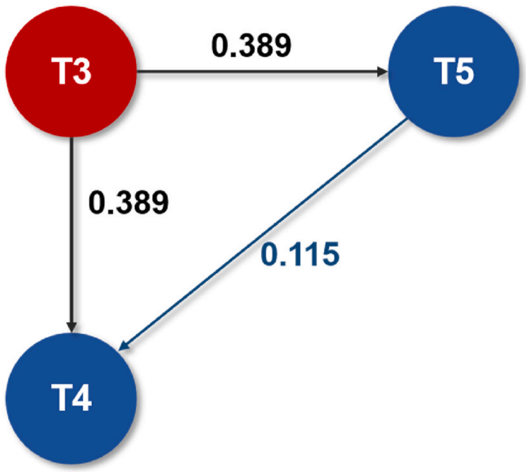

Fig. 7. Simplified layout of T3–T5.

Table 7
DIS of T3 based on probability calculations.

Propagation paths	Probability calculation	Hazard level	Product
T3→T4	$0.389 \times (1 - 0.389)$	2	0.475
T3→T5	$0.389 \times (1 - 0.389) \times (1 - 0.115)$	4	0.841
T3→T4 and T5	0.389×0.389	$2 + 4$	0.907
T3→T5→T4	$0.389 \times (1 - 0.389) \times 0.115$	$2 + 4$	0.163
Summation			2.389

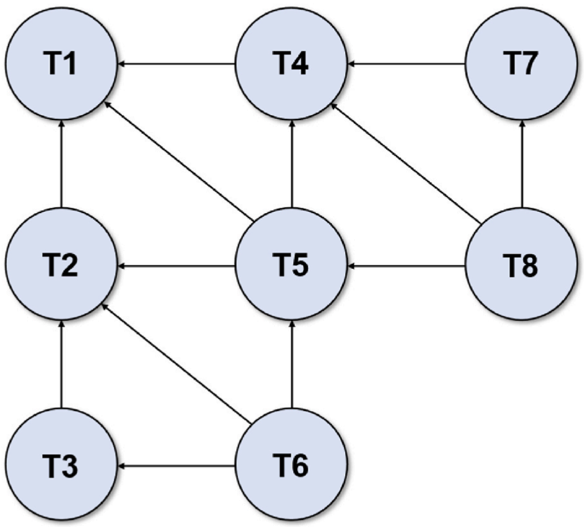

Fig. 8. Schematic of a storage plant consisting of eight tanks of benzene. Each edge represents a heat radiation intensity exceeding 15 kW/m^2 [1].

(3) The domino index considers the hazard level of the installation and reflects the potential consequences of accidents (as depicted in Fig. 2, where tanks had diverse features, indicating the advantage of considering tank hazards).
(4) The method is applicable not only to individual installations but to plant-wide regions.

However, the proposed domino index method only considers a single type of accident in the domino accident chain (i.e., primary explosions leading to secondary explosions, and primary fires leading to secondary fires), and the current methodology may overlook the synergistic effect of pressure waves or thermal radiation, which could potentially bias the assessment of domino accidents. Future research should investigate the synergistic effect and multi-hazard coupling disasters to improve the proposed method. In addition, the

Table 8
Vertex metrics and domino indices for graph in Fig. 8

Tank	Closeness [1]	Betweenness [1]	*DIS*	*DPS*	*EDI*
T1	0.0179	0	0.47	0.12	0.59
T2	0.0207	2.13	3.60	0.71	4.31
T3	0.0245	0.53	6.14	0.14	6.28
T4	0.0207	2.13	3.64	0.69	4.33
T5	0.0303	**3.87**	9.92	**1.36**	11.29
T6	**0.0548**	0	**14.50**	0.14	14.63
T7	0.0245	0.53	6.05	0.18	6.23
T8	**0.0548**	0	**14.47**	0.12	14.59

TNT model and Mudan model employed in the case study are simplified approaches that do not consider wind effects. For more complex conditions, CFD modelling may be a more appropriate choice. Recently, a novel methodology involves the integration of CFD with machine learning, specifically artificial neural networks (ANN) [27,50–52]. Future research could further explore the utilization of ANN models to expedite the assessment of domino effects.

7. Conclusions

This study introduced a set of indices for the rapid quantification of domino effects in chemical plants, using an algorithm based on Monte Carlo simulations. The method obviates the need for probability calculations and is suited for plants with complex layouts. The indices proposed in this paper include *DIS*, *DPS*, *EDI*, and *SDI*. The *DIS* and *DPS* can be used to identify key installations with influential propagation propensity in chemical plants, whereas the *SDI* characterised the overall domino effect and served as a reference for optimising the layouts and screening risks of chemical clusters. In security management, the *EDI* and *SDI* represent the vulnerability of chemical plants to intentional attacks.

The application of the domino indices was demonstrated via two case studies. In the first case, 1000 simulations were sufficient and the required time was 2.57 s. Thus, the approach was shown to be convenient and expeditious. The second case involved five existing storage plants. The higher *SDI* for plant 3 compared to plant 4 (203.73 and 176.02, respectively) demonstrated the influence of regional layout on the domino index proposed in this paper. To verify the efficiency of the domino indices, the results of the proposed method and those reported in the literature were compared. The discrepancy between the two sets of results was 0.2 %, and congruent rankings were obtained from the domino indices and vertex-metric-based method.

In summary, the domino index can be effectively used to quantify domino effects in chemical plants. The proposed algorithm for domino accident modelling, based on Monte Carlo simulations, can account for accident propagation processes and facilitate rapid evaluation. Future enhancements for the domino indices are to address synergies and multi-hazard coupling effects.

Funding

This research did not receive any specific grant from funding agencies in the public, commercial, or not-for-profit sectors.

Data availability statement

The data associated with our study have not been deposited in a publicly available repository. Data will be made available on request.

CRediT authorship contribution statement

Han Gao: Conceptualization, Data curation, Methodology, Writing – original draft. **Yunkai Yang:** Data curation, Investigation. **Hongxing Shi:** Formal analysis, Resources, Supervision, Writing – review & editing.

Declaration of competing interest

The authors declare that they have no known competing financial interests or personal relationships that could have appeared to influence the work reported in this paper.

Acknowledgements

The authors would like to thank Shiyanjia Lab (www.shiyanjia.com) for language editing assistance.

References

[1] N. Khakzad, G. Reniers, Using graph theory to analyze the vulnerability of process plants in the context of cascading effects, Reliab. Eng. Syst. Saf. 143 (2015) 63–73.

[2] C. Chen, G. Reniers, Chemical industry in China: the current status, safety problems, and pathways for future sustainable development, Saf. Sci. 128 (2020), 104741.

[3] N. Alileche, V. Cozzani, G. Reniers, L. Estel, Thresholds for domino effects and safety distances in the process industry: a review of approaches and regulations, Reliab. Eng. Syst. Saf. 143 (2015) 74–84.

[4] A. Necci, V. Cozzani, G. Spadoni, F. Khan, Assessment of domino effect: state of the art and research Needs, Reliab. Eng. Syst. Saf. 143 (2015) 3–18.

[5] V.K. Sharma, CNTFET circuit-based wide fan-in domino logic for low power applications, J. Circ. Syst. Comput. 31 (2021), 2250036.

[6] V. Kajal, K. Sharma, An efficient low power method for FinFET domino OR logic circuit, Microprocess. Microsyst. 95 (2022).

[7] A. Rad, B. Abdolharnidzadeh, T. Abbasi, D. Rashtchian, Freedom II: an improved methodology to assess domino effect frequency using simulation techniques, Process Saf. Environ. Protect. 92 (2014) 714–722.

[8] G. Reniers, V. Cozzani, Domino Effects in the Process Industries, Modelling, Prevention and Managing, Elsevier, Amsterdam, The Netherlands, 2013.

[9] P. Swuste, K. van Nunen, G. Reniers, N. Khakzad, Domino effects in chemical factories and clusters: an historical perspective and discussion, Process Saf. Environ. Protect. 124 (2019) 18–30.

[10] B. Abdolhamidzadeh, T. Abbasi, D. Rashtchian, S.A. Abbasi, Domino effect in process-industry accidents - an inventory of past events and identification of some patterns, J. Loss Prev. Process. Ind. 24 (2011) 575–593.

[11] N. Khakzad, Application of dynamic Bayesian network to risk analysis of domino effects in chemical infrastructures, Reliab. Eng. Syst. Saf. 138 (2015) 263–272.

[12] S.P. Kourniotis, C.T. Kiranoudis, N.C. Markatos, Statistical analysis of domino chemical accidents, J. Hazard Mater. 71 (2000) 239–252.

[13] N. Khakzad, G. Reniers, R. Abbassi, F. Khan, Vulnerability analysis of process plants subject to domino effects, Reliab. Eng. Syst. Saf. 154 (2016) 127–136.

[14] Darran Simon, Madison Park, R. Riess, A Huge Fire at a Texas Chemical Plant Is Out, 4 Days after it Started, CNN, 2019. https://edition.cnn.com/2019/03/20/us/deer-park-itc-plant-fire-wednesday/index.html.

[15] Z. He, W. Weng, A dynamic and simulation-based method for quantitative risk assessment of the domino accident in chemical industry, Process Saf. Environ. Protect. 144 (2020) 79–92.

[16] Z. He, W. Weng, Synergic effects in the assessment of multi-hazard coupling disasters: fires, explosions, and toxicant leaks, J. Hazard Mater. 388 (2020), 121813.

[17] C. Chen, G. Reniers, N. Khakzad, A thorough classification and discussion of approaches for modeling and managing domino effects in the process industries, Saf. Sci. 125 (2020).

[18] V. Cozzani, G. Gubinelli, E. Salzano, Escalation thresholds in the assessment of domino accidental events, J. Hazard Mater. 129 (2006) 1–21.

[19] F.I. Khan, S.A. Abbasi, Models for domino effect analysis in chemical process industries, Process Saf. Prog. 17 (1998) 107–123.

[20] V. Cozzani, E. Salzano, The quantitative assessment of domino effects caused by overpressure. Part I. Probit models, J. Hazard Mater. 107 (2004) 67–80.

[21] G. Landucci, G. Gubinelli, G. Antonioni, V. Cozzani, The assessment of the damage probability of storage tanks in domino events triggered by fire, Accid. Anal. Prev. 41 (2009) 1206–1215.

[22] E.D. Mukhim, T. Abbasi, S.M. Tauseef, S.A. Abbasi, Domino effect in chemical process industries triggered by overpressure-Formulation of equipment-specific probits, Process Saf. Environ. Protect. 106 (2017) 263–273.

[23] M.G. Zhang, J.C. Jiang, An improved probit method for assessment of domino effect to chemical process equipment caused by overpressure, J. Hazard Mater. 158 (2008) 280–286.

[24] L. Ding, F. Khan, R. Abbassi, J. Ji, FSEM, An approach to model contribution of synergistic effect of fires for domino effects, Reliab. Eng. Syst. Saf. 189 (2019) 271–278.

[25] L. Ding, F. Khan, J. Ji, A novel vulnerability model considering synergistic effect of fire and overpressure in chemical processing facilities, Reliab. Eng. Syst. Saf. 217 (2022), 108081.

[26] A. Rum, G. Landucci, C. Galletti, Coupling of integral methods and CFD for modeling complex industrial accidents, J. Loss Prev. Process. Ind. 53 (2018) 115–128.

[27] Q. Li, S. Zhou, Z. Wang, Quantitative risk assessment of explosion rescue by integrating CFD modeling with GRNN, Process Saf. Environ. Protect. 154 (2021) 291–305.

[28] X. Li, G. Chen, K. Huang, T. Zeng, X. Zhang, P. Yang, M. Xie, Consequence modeling and domino effects analysis of synergistic effect for pool fires based on computational fluid dynamic, Process Saf. Environ. Protect. 156 (2021) 340–360.

[29] G. Landucci, M. Molag, V. Cozzani, Modeling the performance of coated LPG tanks engulfed in fires, J. Hazard Mater. 172 (2009) 447–456.

[30] Y. Xu, G. Reniers, M. Yang, S. Yuan, C. Chen, Uncertainties and their treatment in the quantitative risk assessment of domino effects: classification and review, Process Saf. Environ. Protect. 172 (2023) 971–985.

[31] D.F. Bagster, R.M. Pitblado, The Estimation of domino incident frequencies - an approach, Process Saf. Environ. Protect. 69 (1991) 195–199.

[32] P.G. George, V.R. Renjith, Bayesian estimation and consequence modelling of deliberately induced domino effects in process facilities, J. Loss Prev. Process. Ind. 69 (2021), 104340.

[33] N. Khakzad, P. Amyotte, V. Cozzani, G. Reniers, H. Pasman, How to address model uncertainty in the escalation of domino effects? J. Loss Prev. Process. Ind. 54 (2018) 49–56.

[34] T. Zeng, G. Chen, Y. Yang, P. Chen, G. Reniers, Developing an advanced dynamic risk analysis method for fire-related domino effects, Process Saf. Environ. Protect. 134 (2020) 149–160.

[35] C. Chen, G. Reniers, N. Khakzad, Integrating Safety and Security Resources to Protect Chemical Industrial Parks from Man-Made Domino Effects: A Dynamic Graph Approach, Reliability Engineering & System Safety, 2019, p. 191.

[36] N. Khakzad, G. Landucci, G. Reniers, Application of graph theory to cost-effective fire protection of chemical plants during domino effects, Risk Anal. 37 (2017) 1652–1667.

[37] K. Huang, G. Chen, F. Khan, Vulnerability assessment method for domino effects analysis in chemical clusters, Process Saf. Environ. Protect. 164 (2022) 539–554.

[38] K. Huang, G. Chen, F. Khan, Y. Yang, Dynamic analysis for fire-induced domino effects in chemical process industries, Process Saf. Environ. Protect. 148 (2021) 686–697.

[39] C. Chen, G. Reniers, L. Zhang, An innovative methodology for quickly modeling the spatial-temporal evolution of domino accidents triggered by fire, J. Loss Prev. Process. Ind. 54 (2018) 312–324.

[40] V. Cozzani, A. Tugnoli, E. Salzano, The development of an inherent safety approach to the prevention of domino accidents, Accid. Anal. Prev. 41 (2009) 1216–1227.

[41] N. Khakzad, F. Khan, P. Amyotte, V. Cozzani, Domino effect analysis using Bayesian networks, Risk Anal. 33 (2013) 292–306.

[42] G.L.L. Reniers, A. Audenaert, Preparing for major terrorist attacks against chemical clusters: intelligently planning protection measures w.r.t. domino effects, Process Saf. Environ. Protect. 92 (2014) 583–589.

[43] J. Zhou, G. Reniers, V. Cozzani, Improved probit models to assess equipment failure caused by domino effect accounting for dynamic and synergistic effects of multiple fires, Process Saf. Environ. Protect. 154 (2021) 306–314.

[44] B. Abdolhamidzadeh, T. Abbasi, D. Rashtchian, S.A. Abbasi, A new method for assessing domino effect in chemical process industry, J. Hazard Mater. 182 (2010) 416–426.

[45] State Administration for Market Regulation (Samr), Standardization administration of the people's Republic of China (SAC), Identification of major hazard installations for hazardous chemicals. GB18218–2018, China (2018).

[46] V. Cozzani, G. Gubinelli, G. Antonioni, G. Spadoni, S. Zanelli, The assessment of risk caused by domino effect in quantitative area risk analysis, J. Hazard Mater. 127 (2005) 14–30.
[47] E. Salzano, G. Antonioni, G. Landucci, V. Cozzani, Domino effects related to explosions in the framework of land use planning, LP2013 - 14th Symposium on Loss Prevention and Safety Promotion in the Process Industries I and II (2013) 787–792.
[48] Mudan, Thermal radiation hazards from hydrocarbon pool fires, Prog. Energy Combust. Sci. 10 (1984) 59–80.
[49] K.S. Mudan, Geometric view factors for thermal radiation hazard assessment, Fire Saf. J. 12 (1987) 89–96.
[50] S. Zhou, Z. Wang, Q. Li, A fusing NS with NN model for the consequence prediction of vapor cloud explosion, Process Saf. Environ. Protect. 149 (2021) 698–710.
[51] J. Li, Q. Li, H. Hao, L. Li, Prediction of BLEVE blast loading using CFD and artificial neural network, Process Saf. Environ. Protect. 149 (2021) 711–723.
[52] L. Peng, X. Huang, J. Chen, P. Yang, C. Xing, C. Zhao, A method for real-time estimation of gas leakage flow from leakage source based on point detection data, J. Loss Prev. Process. Ind. 78 (2022), 104822.